

# Discrimination of crystal types (bcc, fcc, hcp) using anisotropic scaling indices and bond order parameters

Alex Hartmann

DLR Oberpfaffenhofen, group complex plasmas

09 September 2015

# Table of Contents

Introduction: scaling indices, bond order parameters, crystal types

Quality of discrimination between crystal types: comparison of scaling indices and bond order parameters

From artificially created to unknown data sets

Results for experimental data sets (3D)

Results for experimental data sets (2D)

## Scaling indices - introduction [3]

In a  $n$ -dimensional point distribution containing  $N$  points  $\{\vec{x}_i\}$  with  $i = 1 \dots N$

the scaling index  $\alpha_i(r)$  of point  $i$  gives information about the scaling behaviour of the neighborhood of point  $i$

meaning how the number of neighboring points  $N_{neighbors}$  surrounding point  $i$  scales with a radius-like parameter  $r$ .

This can be seen as a local dimensionality:  $N_{neighbors,i}(r) \sim r^{\alpha_i(r)}$

## Scaling indices - introduction

$\rho_i(r)$  denotes the cumulative point distribution function dependent on a shaping function  $s_r(d_{ij})$ .  $d_{ij}$  means a distance measure between points  $i$  and  $j$ .

$$\rho_i(r) = \sum_{j=1}^N s_r(d_{ij})$$

$$\rho_i(r) \sim r^{\alpha_i(r)} \quad \rightarrow \quad \alpha_i(r) = \frac{\partial \ln \rho_i}{\partial \ln r}$$

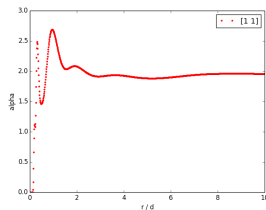
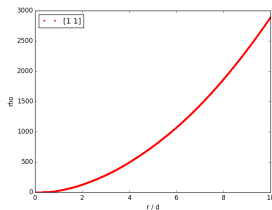
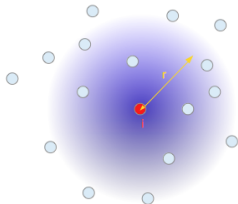
$$d_{ij} = \left( \sum_{p=1}^n (x_{i,p} - x_{j,p})^2 \right)^{\frac{1}{2}}$$

# Scaling indices - differentiable shaping function

point distribution function  $\rho(r)$  with exponential shape:

$$\rho_i(r) = \sum_{j=1}^N e^{-(\frac{d_{ij}}{r})^q}$$

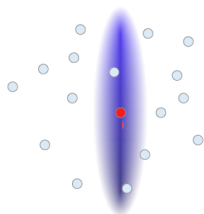
$$\alpha_i(r) = \frac{\partial \ln \rho_i}{\partial \ln r} = \frac{\sum_{j=1}^N q \left(\frac{d_{ij}}{r}\right)^q e^{-(\frac{d_{ij}}{r})^q}}{\sum_{j=1}^N e^{-(\frac{d_{ij}}{r})^q}}$$



# Scaling indices - anisotropic distance measure

Set of  $n$  weighting factors  $\lambda$ 's:  $\{\lambda_1, \dots, \lambda_n\}$   
for  $n$  dimensions

$$d_{ij} = \left( \sum_{p=1}^n \lambda_p (x_{i,p} - x_{j,p})^2 \right)^{\frac{1}{2}}$$



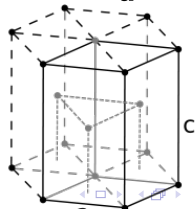
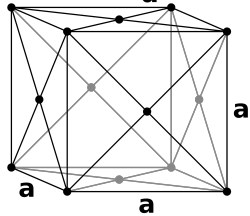
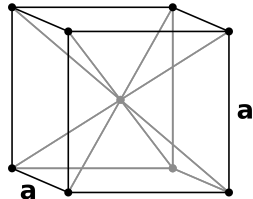
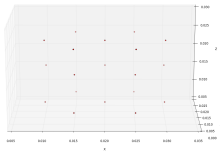
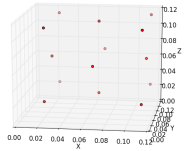
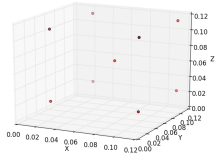
3D:  $(\lambda_1, \lambda_2, \lambda_3) = (1, 9, 9), \dots$  lead to cigar-like shape of  $\rho$  and  
 $(\lambda_1, \lambda_2, \lambda_3) = (1, 1, 9), \dots$  lead to discus-like shape of  $\rho$

So you get a set  $\{\alpha_i\}$ , one for each spatial direction (in algorithm: at least 3), for each shape (cigar-like and discus-like) and for each radius (in algorithm: 10 or 100 steps). This results in a high-dimensional  $\alpha$ -space.

## Bond order parameters [4]

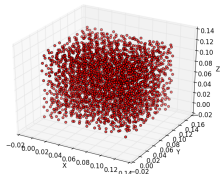
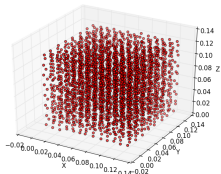
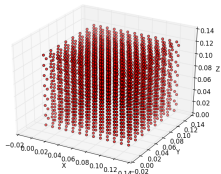
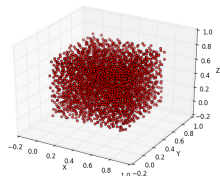
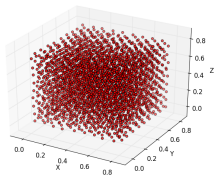
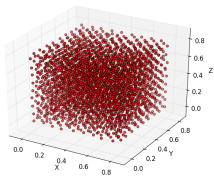
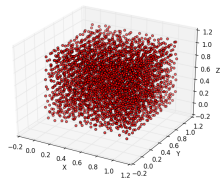
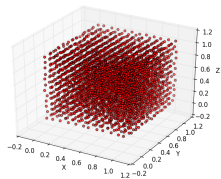
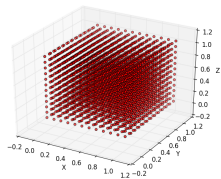
- ▶ Local invariants, not dependent on orientation and scaling
- ▶ For all points of a distribution: in spherical coordinates, calculate  $\phi$  and  $\theta$  between points and next neighbors (nn)
- ▶ Denote:  $Q_{lm} \equiv Y_{lm}$ ,  $l, m =$  degree, order of Legendre pol.:  
 $l \geq 0, \quad -l \leq m \leq l$
- ▶  $Q_l = \left( \frac{4\pi}{2l+1} \sum_{m=-l}^l |\bar{Q}_{lm}|^2 \right)^{\frac{1}{2}}, \quad \bar{Q}_{lm} = \frac{1}{N_{nn}} \sum_{nn} Q_{lm}$
- ▶ Calculate  $Q_4$  and  $Q_6$

# crystal types





# 3D crystalline point dist. with Gaussian noise

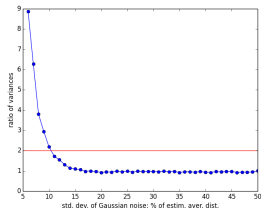
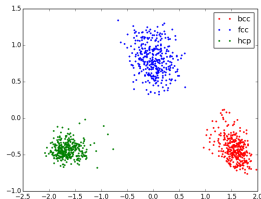


The following plots show the calculated scaling indices  $\alpha$  and the calculated bond order parameters  $Q_4$ ,  $Q_6$  of all points of the distribution visualized as points in the respective parameter space ( $\alpha$ -space or Q-space), in a 2D plane. Since the  $\alpha$ -space is high-dimensional, for visualization reasons a principal component analysis was done and only the first and second principal components are shown.

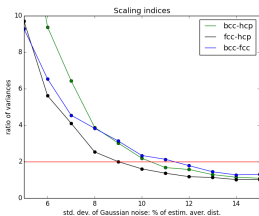
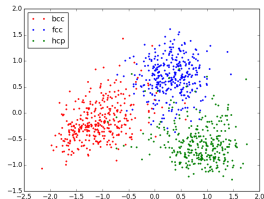
The following graphs show the ratio of the total variance of all the points in the parameter-space divided by the variance of the points referring to only one of the crystal types bcc, fcc or hcp (or their maximum, respectively). The horizontal red line marks the ratio of variances equaling 2.

# 3D crystalline point dist. with Gaussian noise, sca.ind.

noise level: 5%d

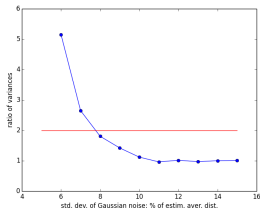
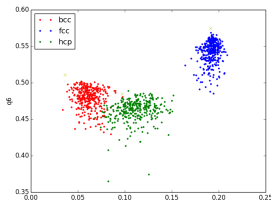


noise level: 10%d

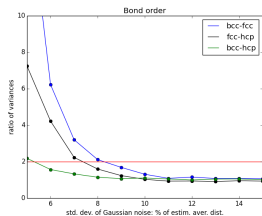
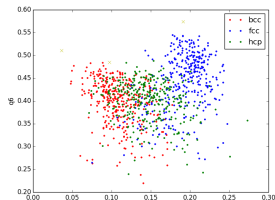


# 3D crystalline point dist. with Gaussian noise, bond order

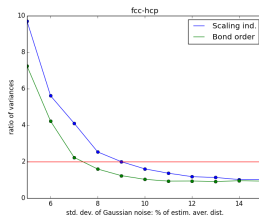
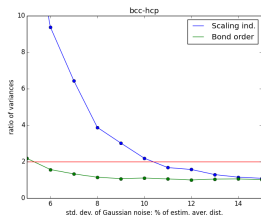
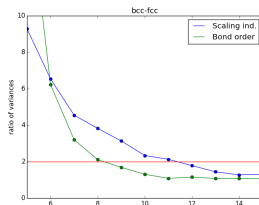
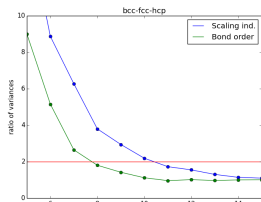
noise level: 5%d



noise level: 10%d



# Comparison scaling indices - bond order parameters



# From artificially created to unknown data sets

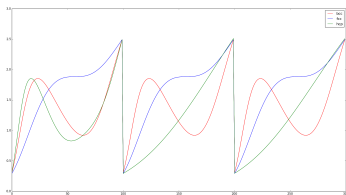
Unknown data sets: no a priori information about crystal types and sizes contained in the point distribution

- ▶ Algorithm needs to be scaling free: initial and final  $r$  for  $r - \alpha(r)$ -curve cannot be fixed a priori
- ▶ Reasonable criterion for denoting a local structure crystalline

# From artificially created to unknown data sets

## Algorithm:

- ▶ first part: calculation of the sets  $\{\alpha_i(r)\}$  for each point  $i$  in the range  $[r_{ini}, r_{fin}]$ , where  $\alpha(r_{ini}) = 0.3$  and  $\alpha(r_{fin}) = 2.5$  (iteration). This range offers a good chance for discrimination between crystal types bcc, fcc and hcp.
- ▶ The set templates  $\{\alpha_{bcc}(r)\}$ ,  $\{\alpha_{fcc}(r)\}$ ,  $\{\alpha_{hcp}(r)\}$  for perfect bcc-, fcc- and hcp-like point distributions are known



# From artificially created to unknown data sets

- ▶ Second part: detect crystalline structures. Criterion needed.
- ▶ “Crystalline”: local structure with similar neighboring structures (at a fixed point of time)
- ▶ “Similar”: average  $\Delta^\alpha$  of some point  $i$  to neighbors  $j$  below certain threshold:  $\frac{1}{N_{neigh}} \sum_{j=1}^{N_{neigh}} \Delta_{i,j}^\alpha < \text{threshold}$
- ▶ Distance in  $\alpha$ -space between points  $i$  and  $j$ :  
 $\Delta_{ij}^\alpha = \sum_{k=1}^{n_{par}} (\alpha_{i,k} - \alpha_{j,k})^2$  with  $n_{par}$  being the dimensionality of the  $\alpha$ -space.
- ▶ The threshold is fixed by the following decision:

low noise data set	$\xrightarrow{!}$	purely crystallin
high noise data set	$\xrightarrow{!}$	no crystals

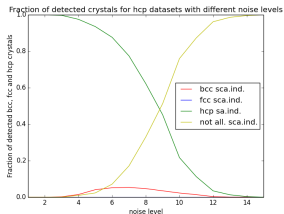
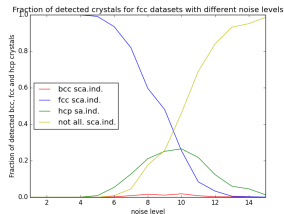
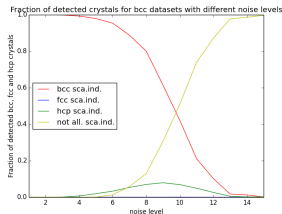
- ▶ For crystalline structures: allocate to bcc, fcc or hcp depending on similarity to templates:  $\min \left( \Delta_{i,bcc}^\alpha, \Delta_{i,fcc}^\alpha, \Delta_{i,hcp}^\alpha \right)$



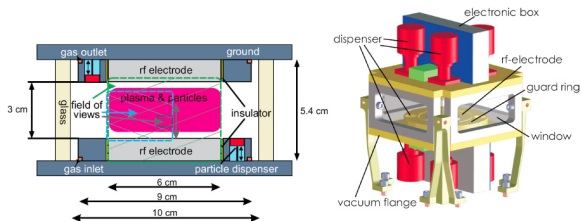
# Results for artificially created data sets

Originally only perfect bcc, fcc or hcp + Gaussian noise  
std.dev.: 1% - 15% average point distance  $d$

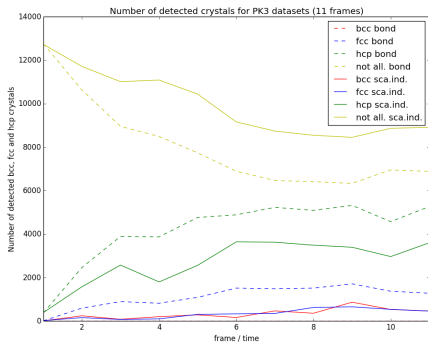
Basis for defining threshold: at the noise level 15%  $d$  all local structures shall be allocated to “non crystalline”.



# Results for experimental PK-3-plus [5] data sets



- ▶ 11 time frames with each about 20000 points in a thin layer
- ▶ Analyses done with bond order parameters method and scaling indices method
- ▶ Analysis with bond order method only for fcc and hcp
- ▶ Next frame shows plot of the time evolution of the numbers of bcc, fcc and hcp for scaling indices method and bond order parameters method in comparison



- ▶ Similar in both methods: number of hcp and fcc in Scan 1: no fcc and a bit of hcp. The behaviour over time of the number of crystals.
- ▶ Different: There is an overall gap between the numbers of crystals. Scaling indices method detects less crystals; despite the quality of discrimination being better for high noise data sets. Reason for this might be the stability criterion in the algorithm.

# Algorithm and results for two-dimensional data sets

- ▶ Improved algorithm: sensible on spatial orientation of the crystals
- ▶ Second data set: “recryst” meaning recrystallization obtained from experiments [[1], p. 13ff, 73ff]
- ▶ Third data set: “melt” meaning melting obtained from a simulation [2]

# Algorithm and results for two-dimensional data sets

Movies of “melt” and “recryst”

To do next:

- ▶ Comparison of results in detail, e.g. intersections and differences in allocations
- ▶ Inclusion of time evolution in detection algorithm
- ▶ Improvement by making the algorithm sensitive on spatial orientation also for 3D



Christina Knapek.

Phase transitions in two-dimensional complex plasmas.  
2010.



I. Laut, C. R  th, S. Zhdanov, V. Nosenko, L. Cou  del, and  
H. M. Thomas.

Synchronization of particle motion in compressed  
two-dimensional plasma crystals.  
*EPL*, 110(65001), 2015.



C. R  th, R. Monetti, J. Bauer, I. Sidorenko, D. M  ller,  
M. Matsuura, E.-M. Lochm  ller, P. Zysset, and F. Eckstein.

Strength through structure: visualization and local assessment  
of the trabecular bone structure.  
*New J. Phys.*, 10(125010), 2008.



P. J. Steinhardt, D. R. Nelson, and M. Ronchetti.

Bond-orientational order in liquids and glasses.  
*Phys. Rev. B*, 28(784), 1983.



H. M. Thomas, G. E. Morfill, V. E. Fortov, A. V. Ivlev, V. I. Molotkov, A. M. Lipaev, T. Hagl, H. Rothermel, S. A. Khrapak, R. K. Suetterlin, M. Rubin-Zuzic, O. F. Petrov, V. I. Tokarev, and S. K. Krikalev.

Complex plasma laboratory PK-3 Plus on the international space station.

*New J. Phys.*, 10(033036), 2008.